J Appl Electrochem (2008) 38:743–749
DOI 10.1007/s10800-008-9503-9

ORIGINAL PAPER

Oxidation of some aliphatic polyols on anodically deposited MnO_2

**Debasmita Das · Purabi Rani Samaddar ·
Pratik Kumar Sen · Kaushik Das**

Received: 25 September 2007 / Revised: 22 January 2008 / Accepted: 28 January 2008 / Published online: 13 February 2008

Abstract Galvanostatic steady state current potential measurements were carried out for oxidation of a series of aliphatic alcohols having varying number of hydroxyl groups. The anodically deposited layer of MnO_2 on platinum was used as the electrode material. The deposit was characterised by scanning electron microscopy (SEM), energy dispersive X-ray analysis (EDAX) and electrode potential measurements. The catalytic role of MnO_2 in the electrooxidation of alcohols was indicated by the chronopotentiograms and the cyclic voltammograms. An analysis of the electrochemical data indicated a catalytic EC mechanism in which Mn (V) is generated electrochemically and consumed chemically in succession. Based on this and the hydrogen bonding interaction between alcoholic hydroxyl groups and MnO_2 layer, a mechanism was proposed which accounts for the variation in the observed electrochemical reaction orders. Tafel behaviour was found to be followed only approximately. Current efficiency of the electrochemical oxidation of polyols was studied. Replacement of platinum by carbon as current collector was found to leave the electrocatalytic activity of the MnO_2 deposit practically unaltered.

Keywords Polyol oxidation · Electrocatalysis · Electrodeposition · MnO_2 electrode · Electrochemical reaction order · Mechanism

1 Introduction

Electrochemical oxidation of organic molecules has several possible applications. It can be used to develop suitable sensors for analytical purposes; it is of prime importance in fuel cell research where organic molecules are used as fuels; it may also be employed as a convenient technique for obtaining useful and desired products selectively. Even in pollution control electrochemical oxidation can be used to reduce the oxygen demand of the effluent within a short time so that the treated solution becomes suitable for discharge into the natural environment. All these applications are relevant for alcohols, both mono-ols and poly-ols. Indeed, the development of the direct alcohol fuel cell (DAFC) [1–6] has been one of the most active areas of research over the last two decades. Also, amperometric detection of alcohols has emerged as an area of considerable research interest [7–12]. Electrochemical oxidation of alcohols is generally carried out in either acidic or alkaline media on highly expensive noble metals and their composites supported on various substrates. Undoubtedly, it will be advantageous if a cheaper electrocatalyst can be developed for this purpose which can work in neutral media.

We have recently explored the possibility of using MnO_2 as an electrocatalyst for carbohydrate oxidation [13, 14]. Manganese exhibits a wide range of higher oxidation states and such oxo-manganese species are generally strong chemical oxidants. Repeated switching between two such states at an electrode can give rise to an anodic current in which the net result is the oxidation of an organic molecule present in the electrolyte. This expectation was substantiated by results obtained using both electrolytically and chemically prepared layers of MnO_2 as electrocatalyst. In the present paper we report findings on the electrochemical oxidation of a series of aliphatic alcohols with varying number of hydroxyl groups and hydrocarbon chain length, employing anodic deposits of MnO_2 as electrode material. The alcohols chosen were propane-1,2-diol (PD), ethanediol

---

D. Das · P. R. Samaddar · P. K. Sen · K. Das (✉)
Department of Chemistry, Jadavpur University,
Kolkata 700 032, India
e-mail: kdas@chemistry.jdvu.ac.in

(ED) and glycerol (G), along with propan-1-ol (P) for comparison. There are earlier reports on the oxidation of methanol on mixed oxides of Mn with Ni [15] and Ru [16] and also on WO_3 [17, 18].

2 Experimental

A platinum (Pt) wire was taken as the support for anodic deposition of MnO_2 layers from 1 M $MnSO_4$ solution at 6 mA cm^{-2} for 30 min. The galvanostatic current potential data for oxidation of various alcohols from solutions of different compositions with 0.25 M Na_2SO_4 as the supporting electrolyte on MnO_2/Pt electrodes were determined at different applied current densities within the range 0.08–1.5 mA cm^{-2} by using a constant current source (DB-300, DB Electronics, India) and a digital multimeter (DM 6104B, EC, India). Chronopotentiometry and cyclic voltammetry were carried out by using a Ministat (AEW2-10, Sycopel Scientific Ltd., U.K.). Potentials were measured with respect to a saturated calomel electrode (SCE).

Electrode surface microstructures were examined with the help of a scanning electron microscope (JEOL 6360, Japan). The surface composition was obtained from energy dispersive X-ray analysis (INCA X-Stream Oxford Instruments, U.K). The chemicals used were of AR grade. All the experiments were carried out at room temperature (30 ± 2 °C)

3 Results and discussion

3.1 Characterisation of the deposited MnO_2 layer

Potential measurement of the MnO_2/Pt electrode and its dependence on both pH and Mn^{2+} concentration were found to agree fairly well with the following redox process

$$MnO_2 + 4H^+ + 2e \rightarrow Mn^{+2} + 2H_2O$$

The standard electrode potential was calculated to be 1.30 V against the literature value of 1.23 V vs. SHE [19]. This showed that the deposit predominantly consisted of MnO_2, although incorporation of a small amount of SO_4^{2-} in the MnO_2 matrix cannot be ruled out. In fact, the composition of the deposited layer in terms of atom %, as obtained from EDAX, included S (1.5–2.5%) in addition to Mn (20–25%) and O (70–80%). The SEM picture (Fig. 1) shows the deposit to be amorphous and of smooth texture with fine cracks. There are also signs of crystallites in the growing regions. The poorly crystalline nature of electrolytic MnO_2, believed to be γ-MnO_2, has been reported earlier [20].

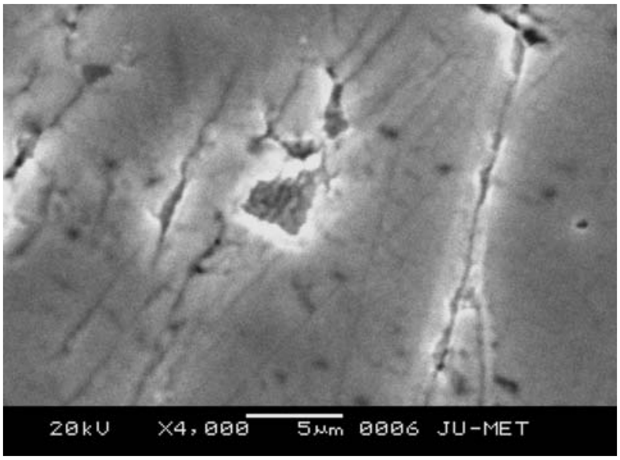

Fig. 1 SEM photograph of the MnO_2 deposit

3.2 Effect of the deposited MnO_2 layer on alcohol oxidation

Galvanostatic current–potential measurements show that the steady state potentials for alcohol oxidation at fixed current densities are in general ~0.6–0.8 V more positive on bare Pt than on MnO_2/Pt. This primarily indicates that the electrocatalytic activity of MnO_2/Pt for alcohol oxidation is substantially greater than that of Pt. This must be due to the fact that the alcohol molecules are sterically hindered from undergoing dissociative adsorption at the carbon atoms bearing the hydroxyl groups, which is generally considered as the first step in the oxidation of lower mono-ols like methanol and ethanol on Pt based electrocatalysts. On the other hand, in the case of poly-ols the possibility of adsorption at the electrode surface through hydrogen bonding becomes important. However, other reasons behind the observed low electrocatalytic activity of Pt cannot be ruled out, e.g., (i) the polycrystalline and non-dispersed nature of the material used in the present work, (ii) the absence of a suitable co-atom like Ru to expedite the alcohol oxidation process and (iii) the use of neutral medium instead of an acidic or an alkaline one.

The enhancement of the oxidation kinetics by deposition of MnO_2 can be interpreted by the possibility of involvement of some manganese species with an oxidation state greater than +4, which is continuously generated by electron transfer and consumed chemically during the oxidation process. Thus MnO_2 acts not only as a simple electron sink but also as a catalyst and the overall process can be considered to follow a catalytic EC mechanism. The production of a higher valent manganese species during oxidation has been reported earlier [21, 22].

The catalytic role of the MnO_2 layer deposited on Pt was indicated by the considerable lengthening of the chronopotentiometric transition time in the presence of the alcohol molecules, while the plateau potential before the transition remained more or less the same (Fig. 2). Also, the anodic scans in the cyclic voltammograms of the MnO_2/Pt electrodes (Fig. 3) showed higher peak currents in the presence of alcohols than in blank, the peak potential being shifted to slightly more positive values. Thus both the chronopotentiometric and the cyclic voltammetric data support the proposed catalytic EC mechanism. However, both the transition time and the anodic peak currents were found to increase in the order P < PD < ED < G.

3.3 Electron transfer process at the MnO_2/Pt electrode

To understand the electron transfer process more quantitatively, the cyclic voltammograms (CV) and the chronopotentiograms (CP) of the MnO_2/Pt electrode in absence of the alcohol molecules need to be analyzed. The peak currents in the CVs were found to increase non-linearly to a limiting value with potential scan rate (v). On the other hand, the CP transition times (τ) to oxygen evolution region were found to increase so rapidly with decreasing applied current densities (j) that the transition could not be obtained within a practically reasonable period of time at sufficiently low values of j. Similar results were obtained earlier for a chemically prepared MnO_2 deposit [14] and analyzed by considering the generation of a reactive Mn species with an oxidation state greater than +4, denoted by Mn(*), and its subsequent disproportionation.

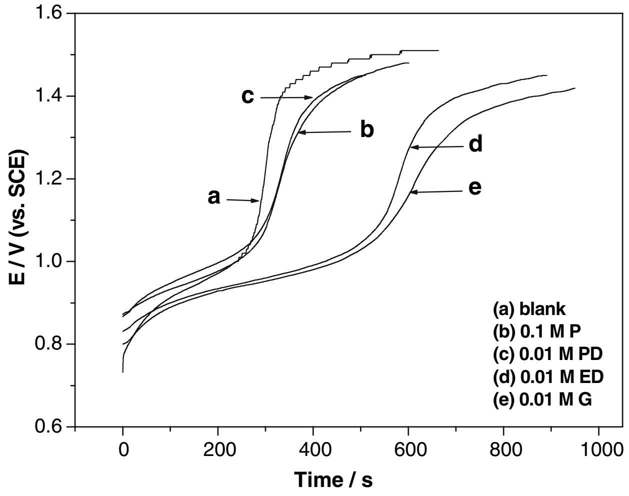

Fig. 2 Anodic chronopotentiograms at 1 mA cm^{-2} on MnO_2/Pt electrodes in absence (blank) and presence of different alcohols

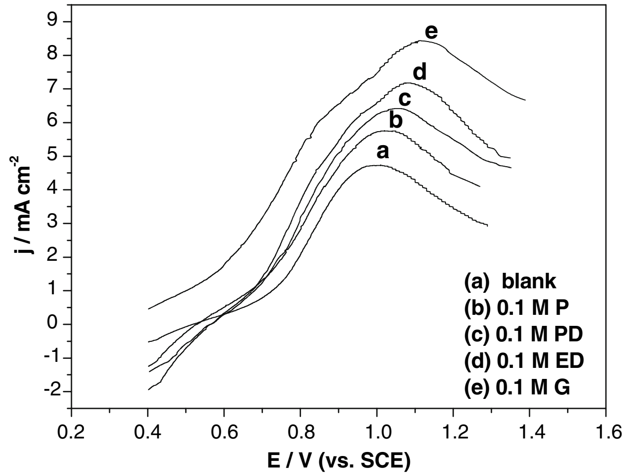

Fig. 3 Anodic scans in the cyclic voltammograms of MnO_2/Pt electrodes in absence (blank) and presence of different alcohols at 0.02 V s^{-1}

The basic electron transfer process is

$$\mathrm{Mn(IV)} - ne \rightarrow \mathrm{Mn}(*) \qquad (1)$$

Let N_o be the initial surface density of Mn (IV) sites in the deposit while N_t and θ_t denote respectively the surface density and fraction of Mn atoms present as Mn(*) at any instant t during current flow. However, the Mn (*) species is likely to be unstable unless it is Mn (VII) and is expected to be converted partially back to Mn (IV) by disproportionation. Thus in the case of CV, θ_t should be less than the value obtained from the Nernst equation by using the electrode potential E_t at time t. This difference in θ_t leads to an anodic overpotential arising out of the disproportionation of Mn (*). The magnitude of this overpotential should, therefore, be a function of both the fraction of Mn (*) in the layer at time t (θ_t) and also the rate of generation of fresh Mn (*). The latter must be related to the anodic potential sweep rate (v) employed. Now, assuming this overpotential to be simply proportional to the product $v\theta_t$, as a first approximation, as in a second order rate equation, one can write

$$E_t = E^0 + \frac{RT}{nF}\ln\frac{\theta_t}{1-\theta_t} + kv\theta_t \qquad (2)$$

After differentiation with respect to t and noting that $v = dE/dt$, we get

$$v = \left(\frac{1}{b\theta_t(1-\theta_t)} + kv\right)\left(\frac{d\theta_t}{dt}\right) \qquad (3)$$

Now, the current density j_t at time t is given by

$$j_t = nFN_0\left(\frac{d\theta_t}{dt}\right) \qquad (4)$$

At current peak $(dj_t/dt) = 0$, while $(d\theta_t/dt) \neq 0$. Using these conditions along with Eqs. 3 and 4, one obtains $\theta_t = ½$ at peak current j_p. The expression for j_p is found to be

$$j_p = \frac{S_{CV}v}{1 + \frac{1}{4}k\left(\frac{nF}{RT}\right)v} \qquad (5)$$

where S_{CV} stands for $[¼\, nFN_o(nF/RT)]$.

Equation 5 gives rise to a limiting behaviour of j_p with increasing v, which justifies the experimental results reported earlier.

Using the same model in case of CP at a certain current density j one can write

$$\frac{d\theta_t}{dt} = \frac{j}{nFN_0} - k'\theta_t \tag{6}$$

where the first and the second terms express the contributions of the generation and the disproportionation of Mn(*) respectively, k' being an appropriate constant.

Integrating Eq. 6 within the limits $t = 0$, $\theta_t = 0$ and $t = \tau$, $\theta_t = 1$ we get

$$j = \left(S_{CP}k'\right)\left[1 - \exp(-k'\tau)\right]^{-1} \tag{7}$$

where S_{CP} stands for $[nFN_o]$.

Equation 7 indicates that, as j approaches $S_{CP}k'$, τ tends to be very high so that the transition does not occur within a reasonable time. The results of CP measurements reported earlier can thus be rationalised. Moreover, combining the expressions for S_{CP} and S_{CV} one can determine n, the number of electrons transferred in step 1, as

$$n = \left(\frac{4RT}{F}\right)\left(\frac{S_{CV}}{S_{CP}}\right) \tag{8}$$

Using the measured j_p at different v and τ at different j (Table 1), S_{CV} and S_{CP} are calculated to be 354 mC V^{-1} cm^{-2} and 42 mC cm^{-2} respectively. These values, when put in Eq. 8, give n = 0.87. As n must be an integer this result indicates the basic electrochemical step 1 to be a one-electron transfer process. Thus it can be concluded that the electrogenerated Mn (*) is actually Mn(V). Indeed the +5 oxidation state is considered to be an important intermediate in the mechanism of the redox process involving different Mn compounds [23]. Although Mn (V) species is stable only in strongly alkaline solutions, in the present case its existence is transitory and, after electrogeneration, it is rapidly consumed either by disproportionation or by reacting with the alcohol molecules.

As stated earlier, both peak current and transition time were found to increase in the presence of the alcohols in solution. This indicates that the extent of accumulation of Mn (V) on the surface, as expressed by θ_t, becomes less in the presence of the alcohols due to the possibility of being converted back to Mn (IV) by the redox reaction between Mn (V) and alcohol molecules. Thus the overall process can be considered to follow a catalytic EC mechanism in which the consumption and the regeneration of the catalyst Mn (IV) remain confined to the electrode surface.

Table 1 (a) Anodic peak currents and potentials (vs. SCE) at different potential scan rates in 0.25 M Na_2SO_4. (b) Chronopotentiometric transition times (τ) and quarter wave potentials ($E_{\tau/4}$) vs. SCE at different current densities in 0.25 M Na_2SO_4

	Potential scan rate/V s^{-1}				
	0.005	0.01	0.02	0.03	0.05
(a)					
j_p/mA cm^{-2}	2.52	3.48	4.88	6.8	10.24
E_p/V	0.97	0.98	0.99	1.04	1.12
	j/mA cm^{-2}				
	1.5	2	4	5	
(b)					
τ/s	240	94	15	6	
$E_{\tau/4}$/V	0.94	0.98	1.02	1.01	

3.4 Variation of electrochemical reaction order

The electrochemical reaction order (ρ) is defined as the slope of the log–log plot of current density (j) vs. concentration (C) at a fixed potential [24]. From such plots (Fig. 4) it is observed that the slopes, i.e., the reaction orders, decrease along the series P > PD > ED > G. All the reaction orders, except for P, were found to be considerably less than unity (Table 2). For electrochemical oxidation of organic compounds it can reasonably be assumed that only the molecules adsorbed onto the electrode surface are capable of undergoing electron transfer. Hence, the rate of reaction is expected to be directly proportional to the surface concentration (C_s) of the adsorbed alcohol molecule and the 'true' reaction order, given by ($d\log j/d\log C_s$) at constant potential, should be unity.

Now, C_s and C are related by the equation $C_s = \frac{kK_{ad}C}{1+K_{ad}C}$ for monolayer adsorption where K_{ad} is the adsorption equilibrium constant and k another appropriate constant.

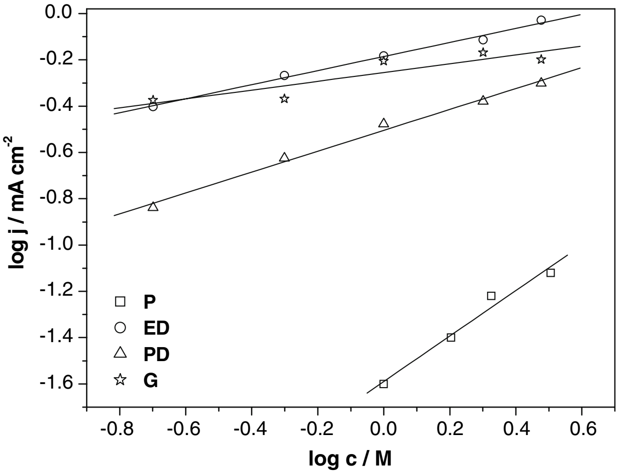

Fig. 4 Log–log plots of oxidation current density vs. alcohol concentration at 0.8 V (vs. SCE) for determination of electrochemical reaction order

Table 2 Electrochemical reaction order (ρ) for oxidation of different molecules on anodically prepared MnO_2/Pt electrode

Molecules	ρ
Propan-1-ol	0.98 ± 0.05
Propane-1,2-diol	0.45 ± 0.05
Ethane diol	0.30 ± 0.05
Glycerol	0.19 ± 0.05

Therefore,

$$\begin{aligned}\rho = \left(\frac{\partial \log j}{\partial \log C}\right)_{potential} &= \left[\left(\frac{\delta \log j}{\delta \log C_S}\right)\left(\frac{\delta \log C_S}{\delta \log C}\right)\right]_{potential} \\ &= 1 - \frac{K_{ad}C}{1 + K_{ad}C} \\ &= \frac{1}{1 + K_{ad}C} < 1\end{aligned}$$

This explains the experimentally observed values of ρ.

Moreover, as the extent of adsorption becomes greater, i.e. for higher K_{ad} values, the reaction order with respect to the solution concentration is also expected to be smaller. The adsorption of the molecules in the present study on the oxide surface is likely to occur via hydrogen bonding between the surface O atom and the hydroxyl groups of the alcohol molecules. With increasing number of –OH groups in the adsorbed molecule the adsorption on the oxide surface is likely to be enhanced from statistical consideration. This is reflected in the observed decrease of electrochemical reaction order from mono-ol to diol to triol.

To explain the observed sequence of the reaction orders for the diols PD and ED, the electron releasing inductive effect of the additional methyl group in the former has to be considered. This effect is expected to decrease the electrostatic charge density at the positive end of the OH dipole near the hydrogen atom. Consequently the hydrogen bond donating ability of PD should be lower than that of ED. This results in a relatively stronger adsorption of ED on the electrode surface than PD. Therefore, the observed reaction order is of lower value in case of ED.

3.5 Steady state current–potential behaviour

A comparison (Fig. 5) of the potential vs. log current density plots for oxidation of different alcohols on MnO_2/Pt shows that the required potentials for a fixed current density decrease in the order P > PD > ED $\approx$ G. An approximate Tafel behaviour is observed, particularly at lower currents. The Tafel slopes increase from ~0.13 to ~ 0.21 V dec^{-1} with increasing hydrogen bond donating ability of the molecules. The gradual increase in the Tafel slopes possibly indicates kinetic complications to some extent due to the progressively stronger adsorption of these molecules onto the electrode surface, as discussed earlier (Sect. 3.4). Thus the results from electrochemical reaction order and Tafel slope measurements appear to be compatible.

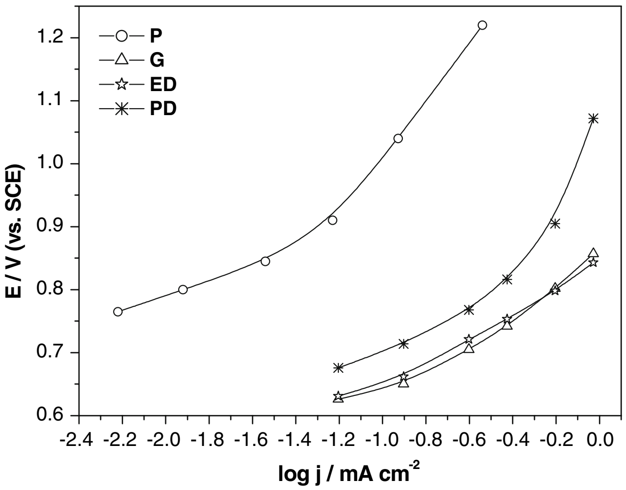

Fig. 5 Tafel plots for oxidation of different alcohols from 1 M solutions on MnO_2/Pt electrode

3.6 Current efficiency of oxidation

Oxidation of the alcohols taken in the present study is expected to primarily produce aldehydic carbonyl groups. Titration with Fehling's solution [25] can thus be utilised to determine the current efficiency with respect to the first stage of oxidation because this analytical technique measures only the aldehyde concentration. Therefore, from the titre values obtained before and after prolonged electrolysis of the alcohol solutions using MnO_2/Pt electrodes, the amount of aldehydes accumulated in the solution can be estimated. The electrolysis experiments were carried out by choosing an appropriate constant current so that the potential remained around 0.9V vs. SCE. The current efficiencies for aldehyde production were found to be ~50% for G and ~40% for both ED and PD. However, the oxidation may proceed beyond the aldehyde stage to the generation of carboxylic acid and CO_2, which are not detectable by Fehling titration. Hence the actual current efficiencies should be higher than the above values.

3.7 Proposed mechanism

On the basis of the above discussion a possible mechanism of electrochemical oxidation of alcohols on MnO_2 layer deposited on Pt may be proposed (Fig. 6) Here Mn = O represents a pair of adjacent Mn and O atoms at the surface of the MnO_2 matrix. In the case of poly-ols, the adsorption

Fig. 6 Proposed mechanism of electrochemical oxidation of alcohols on MnO_2/Pt

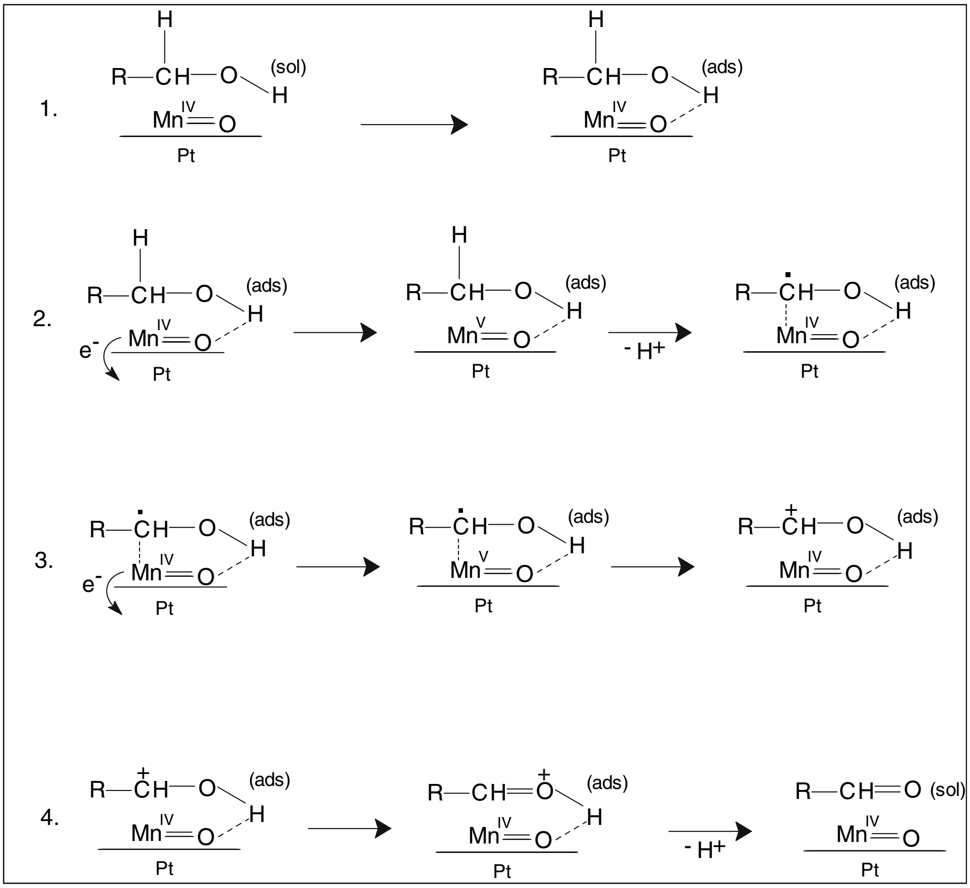

[R≡C_2H_5; CH_2OH; CH_3CHOH; $CH_2(OH)CHOH$]

may also occur through another –OH group adjacent to the one undergoing oxidation. The mechanism remains essentially unchanged, but now the oxidation product can remain adsorbed on the electrode surface. Unless it is desorbed quickly, this particular site becomes unavailable for further oxidation and kinetic complications appear.

3.8 Replacement of platinum by carbon as current collector

Throughout the present study MnO_2 was electrodeposited on Pt substrate so that the deposited layer could be removed easily without affecting the base surface during cleaning. As Pt is highly expensive it would be worthwhile to find out whether the electrocatalytic properties of MnO_2 deposit were maintained on other cheaper substrates. For this purpose carbon current collectors from commercial dry cells were used to prepare MnO_2/C electrodes. The current potential behaviour for oxidation of polyols remained almost unchanged on these electrodes, both qualitatively as well as quantitatively, compared to those obtained on MnO_2/Pt electrodes. Thus, Pt can be replaced by the much cheaper material C as the substrate without any loss in the electrocatalytic activity of the MnO_2 deposit.

4 Conclusions

The electrocatalytic role of anodically deposited MnO_2 in the oxidation of alcohols with multiple hydroxyl groups in a medium of neutral pH has been demonstrated and a possible mechanism has been proposed. The electrocatalysis takes place by successive generation and consumption of a Mn (V) species. Measurements of current efficiencies indicated that oxidation proceeds beyond the aldehyde stage. Instead of Pt, MnO_2 can also be deposited on carbon substrates without affecting its electrocatalytic activity for alcohol oxidation.

Acknowledgment Financial assistance from Defence Research Development Organization (DRDO, India), Jadavpur University and ICCR is gratefully acknowledged. One of the authors (D.D.) thanks J.U. and another (P.R.S.) thanks ICCR for providing research fellowships.

References

1. Kamarudin SK, Daud WRW, Ho SL, Hasran UA (2007) J Power Sources 163:743
2. Antolini E (2007) J Power Sources 170:1
3. Liu H, Song C, Zhang L, Zhang J, Wang H, Wilkinson DP (2006) J Power Sources 155:95
4. Dillon R, Srinivasan S, Arico AS, Antonucci V (2004) J Power Sources 127:112
5. Lamy C, Lima A, LeRhun V, Delime F, Coutanceau C, Léger J-M (2002) J Power Sources 105:283
6. Wasmas S, Kuver A (1999) J Electroanal Chem 461:14
7. Shen PK, Xu C (2006) Electrochem Comm 8:184
8. Casella IG, Gatta M (2002) J Electroanal Chem 534:31
9. Cataldi TRI, Guerrieri A, Casella IG, Desimoni E (1995) Electroanal 7:305
10. Wang J, Taha Z (1991) Anal Chem 62:1413
11. Prabhu SV, Baldwin RP (1989) Anal Chem 61:2258
12. Morrison TN, Schick KG, Huber CO (1980) Anal Chim Acta 120:75
13. Das D, Sen PK, Das K (2006) J Appl Electrochem 36:685
14. Das D, Sen PK, Das K (2007) J Electroanal Chem 611:19
15. Samant PV, Fernandes JB (1999) J Power Sources 79:114
16. Rebello JS, Samant PV, Figueiredo JL, Fernandes JB (2006) J Power Sources 153:36
17. Shukla AK, Ravikumar MK, Arico A, Candiano G, Giordano N, Hamnet A (1995) J Appl Electrochem 25:528
18. Zhang DY, Ma ZF, Wang GZ (2006) Electrochem Solid State Lett 9:685
19. Lurie J (1975) Handbook of analytical chemistry. Mir Publishers, Moscow
20. Rodrigues S, Munichandraiah N, Shukla AK (1998) J Appl Electrochem 28:35 and relevant references therein
21. Rogulski Z, Siwek H, Paleska I, Czerwinski A (2003) J Electroanal Chem 543:175
22. Chun SE, Pyun S, Lee G (2006) Electrochim Acta 51:6479
23. Kemmitt RDW, Peacock RD (1973) The chemistry of manganese, technetium and rhenium, pergamon text in inorganic chemistry, 1st edn. Pergamon Press
24. Gileadi E, Kirowa-Eisner E, Penciner J (1975) Interfacial electrochemistry; an experimental approach. Addison-Wesley Publishing Company, Inc., p 70
25. Vogel AI (1989) Textbook of practical organic chemistry, 5th edn. ELBS, p 1219